Nanotechnology

DOI: 10.1002/ange.200601104

Metallic Striped Nanowires as Multiplexed Immunoassay Platforms for Pathogen Detection**

Jeffrey B.-H. Tok, Frank Y. S. Chuang, Michael C. Kao, Klint A. Rose, Satinderpall S. Pannu, Michael Y. Sha, Gabriela Chakarova, Sharron G. Penn, and George M. Dougherty*

The rapid growth and development in biodetection technology has largely been driven by the emergence of new and deadly infectious diseases and the realization of biological warfare as new means of terrorism.[1,2] To address the need for portable, multiplex biodetection systems, we report here a novel biosensing platform using engineered nanowires as an alternative substrate for sandwich immunoassays (Figure 1 A). The nanowires are built through submicrometer layering of different metals by electrodeposition within a porous alumina template.[3,4] A variety of metals can be deposited: in this study, we employed stripes of gold, silver, and nickel. Owing to the permutations in which the metals can be deposited, a large number of unique yet easily identifiable encoded nanowires can be included in a multiplex array format.

Image processing of an optical reflectance image can enable the stripe pattern to be identified rapidly, while fluorescence images report information on the degree of binding between the antibody-conjugated nanowires and a fluorophore-tagged antigen target. Such nanowires have been utilized to efficiently detect and report both DNA hybridization and immunoassay processes.[5,6] Herein, we demonstrate the feasibility of using multistriped metallic nanowires (Figure 1 A) in a suspended format to enable rapid and sensitive single and multiplex immunoassays for biowarfare agent simulants.

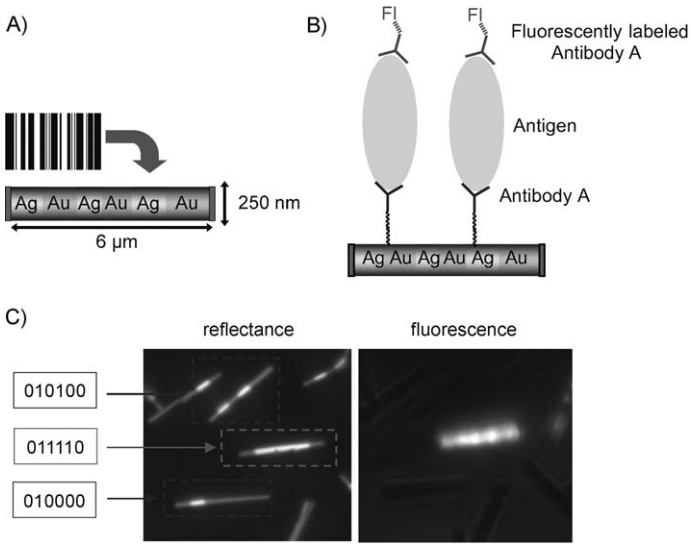

Figure 1. A) Analogy between a conventional barcode and a metallic stripe-encoded nanowire (diameter ≈ 250 nm; length ≈ 6 μm). Ni segments (50 nm) are deposited at both ends on the magnetic nanowire (not drawn to scale). B) Schematic of the sandwich immunoassay performed on a nanowire. C) Post-assay reflectance and fluorescence readout of the nanowires. The identity of the antigen present can be easily identified from the stripe pattern of the nanowires; for example, the fluorescently lit nanowire to which anti-Bg spore Ab was attached has a stripe pattern of 011110 (0 = Au, 1 = Ag). This indicates that Bg spores are present in the test sample mixture. Nanowires with the stripe patterns 010000 (functionalized with anti-Ova Ab) or 010100 (functionalized with BSA; negative control) are not fluorescently lit, thus indicating that the test sample does not contain Ova proteins.

Both the hybridization and kinetics of the capture of the target analyte in solution favor the nanowires over conventional fixed array-based formats. The incorporation of an appropriate ferromagnetic metallic component, for example, Ni, enables the nanoparticles to be manipulated by using magnetic fields.[7–10] To demonstrate the capability of directly detecting potential biological warfare agents in both clinical and environmental samples, a reagent set of three antigens generally accepted for use in simulating actual biothreat agents was chosen. The three nonpathogenic simulants include 1) *Bacillus globigii* (Bg) spores to simulate *Bacillus anthracis* and other bacterial species, 2) RNA MS2 bacteriophage to simulate *Variola* (virus for smallpox) and other pathogenic viruses, and 3) ovalbumin (Ova) protein to simulate protein toxins such as ricin or botulinum toxin. Besides the relative handling safety of these simulants, they were also chosen to reflect the variation in target sizes, ranging from large bacterial spores (≈ 2 μm) to small protein molecules (≈ 2 nm).

[*] Dr. J. B.-H. Tok, Dr. F. Y. S. Chuang, M. C. Kao, Dr. K. A. Rose, Dr. S. S. Pannu, Dr. G. M. Dougherty
Lawrence Livermore National Laboratory
Livermore, CA 94551 (USA)
Fax: (+1) 925-422-3570
E-mail: tok2@llnl.gov
Dr. K. A. Rose
Stanford University
Stanford, CA 94305 (USA)
Dr. M. Y. Sha, Dr. G. Chakarova, Dr. S. G. Penn
Nanoplex Technologies Inc.
Mountain View, CA 94043 (USA)
Dr. F. Y. S. Chuang
NSF Center for Biophotonics Science and Technology
University of California at Davis
Sacramento, CA 95817 (USA)

[**] This work was performed under the auspices of the US Department of Energy by the University of California, Lawrence Livermore National Laboratory, under contract no. W-7405-Eng-48. The authors thank Ian Walton and Scott Norton of Nanoplex Technologies for their assistance in imaging and analysis of the nanowires, and Frances Wong of Nanoplex Technologies for supplying the nanowires. J.B.T. acknowledges the partial support of NIH grant AI065359. Nanoplex Technologies Inc. acknowledges funding from the National Institute of Standards and Technology, Advanced Technology Program Grant (no. 70NANB1H3028).

Supporting information for this article is available on the WWW under http://www.angewandte.org or from the author.

We first analyzed antibody-coated nonmagnetic nanowires containing only Au and Ag segments, using the sandwich immunoassay (Figure 1B). Both single- and multiplex assays were carried out using the panel of biodetection simulants, and the results obtained demonstrated specific, concentration-dependent fluorescence proportional to the amount of target antigen present in solution. Simultaneous analysis of both the reflectance and the fluorescence images of a mixture of three different nonmagnetic nanowires enabled easy identification of the antigen present (Figure 1C). The identity of the antibodies (Abs) was known through analysis of the corresponding stripe pattern of the nanowire to which they were attached. For example, the indicated fluorescent nanowire has a stripe pattern of 011110 (0 = Au and 1 = Ag). Given that anti-Bg spore Ab was attached to this type of nanowire, it is concluded that Bg spore antigens are present in the test sample mixture. At the same time, nanowires with the stripe pattern 010000 which are conjugated with anti-Ova protein Ab are nonfluorescent, thus indicating that the test sample does not contain Ova proteins (stripe pattern 010100, conjugated with BSA, was used as a negative control).

Multiplex titration graphs for Bg spores, Ova protein, and MS2 bacteriophage were obtained upon performing a detailed concentration-dependent titration experiment for each simulant antigen (Figure 2A–C, respectively; data for single assays are not shown). We observed an increase in the fluorescence signal with an increasing concentration of the simulant antigens. There was nonetheless a small corresponding gradual increase in cross-reactivity with other simulants. Employing such steps as increasing the number of washes prior to particle imaging and restricting the number of nanowires loaded in each well (96-well plate utilized) for analysis can reduce the level of cross-reactivity. The number of nanowires loaded in each well should not exceed approximately 1×10^5 in quantity to prevent aggregation of the nanowires during the imaging process. Over the course of approximately 5–10 assays, a signal-to-noise ratio of about 8–12 was consistently observed for the panel of three simulants studied. This observation suggests that the reproducibility of this assay is high.

During the incubation steps, the nanowires have a tendency to settle out of solution, thus the solution was placed on a mixer or vortexed intermittently to maintain active mixing in a suspended format. From the obtained titration curves (Figure 2A–C), the sensitivity, or limit-of-detection (LoD), for the Bg spores, MS2 bacteriophage, and Ova protein was estimated to be 1×10^5 cfu mL^{-1}, 1×10^5 pfu mL^{-1} and 5 ng mL^{-1}, respectively (cfu = colony-forming units; pfu = plaque-forming units). The LoDs estimated for the antigens studied are comparable with other previously reported platforms such as luminex beads and microarrays.[11–13] To directly compare the sensitivity of this nanowire-based immunoassay against ELISA (enzyme-labeled immunosorbant assay), cytokines could be detected in both approaches at concentrations as low as 10 pg mL^{-1} (unpublished data). Interestingly, the sensitivity or LoD of this assay is also directly proportional to the amount of antibody-coated nanowires employed. We observed that when about 1×10^6 nanowires were employed for the detection of cytokine FGF4, the LoD obtained was around 1000 pg mL^{-1}. Upon decreasing the number of nanowires to 1×10^4, there was a corresponding decrease in the LoD to about 10 pg mL^{-1}, which reflects a 100-fold increase (unpublished data). However, the handling of such a small number of nanowires presents a significant challenge during the numerous washing steps. Through a series of optimizing steps to enable an easy-to-implement protocol, we employed approximately 10^8 nanowires in this immunoassay to ensure an optimal LoD and ease in manipulation.

Another approach to enhance the LoD is to ensure that all the capture antibodies are optimally positioned to maximize

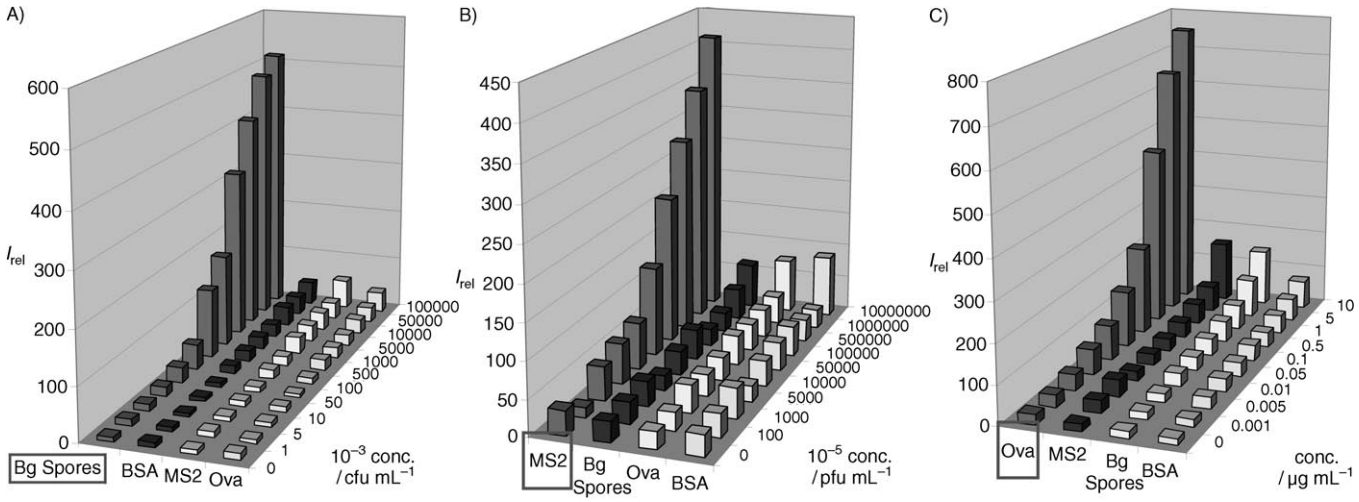

Figure 2. Titration charts of a tetraplex assay consisting of anti-Bg Ab, anti-Ova Ab, anti-MS2 Ab, and BSA-conjugated nanowires versus increasing concentrations of the following simulants: A) Bg spore antigen (from 0 to 1×10^8 cfu mL^{-1}, with 1×10^3 cfu mL^{-1} being the next lowest tested concentration), B) MS2 antigen (from 0 to 1×10^9 pfu mL^{-1}, with 1×10^4 pfu mL^{-1} being the next lowest tested concentration), and C) ovalbumin antigen (from 0 to 1×10 μg mL^{-1}, with 1×10^{-2} μg mL^{-1} being the next lowest tested concentration).

the detection of the antigen. However, owing to the availability of several free amino groups in the capture antibodies, the antibodies may be randomly oriented on the nanowires surface. It was therefore assumed that only a fraction of the conjugated antibodies participate in the antigen-binding event, thus resulting in the observation of a lower LoD value. Additionally, the affinities of the antibodies employed in this study to their respective antigen could also be a factor. Note that both the anti-MS2 and anti-Ova antibodies are polyclonal and may contribute to the high LoD values observed. This indicates that the affinity of the antibody to its antigen is also an important factor to enhance their assay sensitivity.

Second, we investigated if magnetic nanowires are amendable to the above-described immunoassay against the simulated pathogens. As mentioned above, short segments of Ni can confer magnetic properties to nanowire particles. To this end, varying length of Ni segments (25–150 nm) were integrated at both ends of the nanowires and the resulting magnetic properties were investigated. The magnetic easy axis for these disk-shaped segments is perpendicular to the nanowire axis.[14] The particles therefore align perpendicular to the applied magnetic field. It was observed that longer Ni segments result in stronger magnetophoresis but also increased aggregation between the magnetic nanowires after exposure to the magnets during 30 minutes (Figure 3 A and Figure 4), which hinders subsequent imaging. Interestingly, the mobility of the nanowires tipped with 25-nm Ni was an order of magnitude greater than reported values for magnetite-infused polystyrene beads with a diameter of 1 μm used in similar assays.[15,16] Nickel segments with lengths greater than the corresponding diameter exhibit an easy axis parallel to the nanowire axis, causing the particle to align parallel to the magnetic field.[14] This alignment reduces hydrodynamic drag and should further increase particle mobility. Thus, to ensure ease of magnetic manipulation by a magnetic field and minimization of clumping as a result of magnetism, nanowires tipped with 50-nm Ni were chosen for our subsequent immunoassay. The introduction of Ni at the ends helps to ensure both the structural robustness and the decoding process of the nanowires.

Custom electromagnets and several commercially available microfuge tube magnetic separators were investigated for their ability to recover the magnetic nanowires. With a suspended mixture of nanowires tipped with 50 nm Ni, it was observed that all the nanoparticles are able to fully migrate towards the Dynal Biotechnology microfuge tube magnetic separator (Brown Deer, WI) within 4 minutes (Figure 3 B).

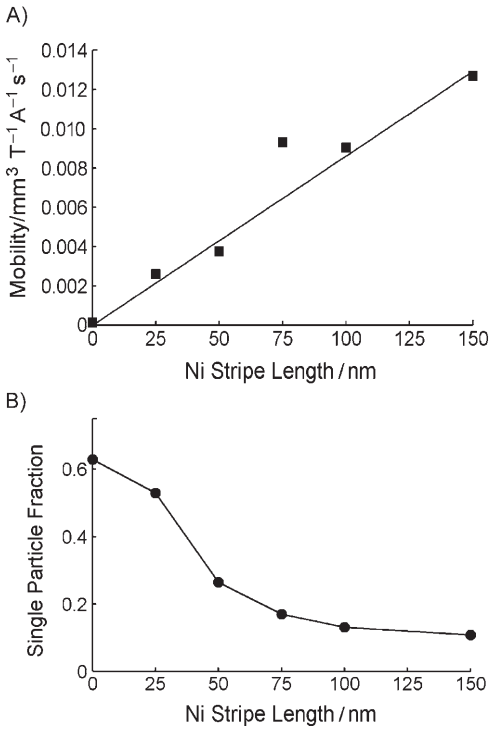

Figure 4. Comparison of characteristics of pure Au nanowires (stripe pattern: 30000003; 0 = Au, 3 = Ni) for various lengths of Ni segments deposited at both ends (total Ni amount is twice the stripe length). A) Magnetophoretic mobility of the nanowires in deionized water, assuming an orientation perpendicular to the direction of motion. Each data point is extracted from measurements of particle velocities for five magnetic energy density values. The solid line shows the approximate linearity of the mobility with the length of the Ni segment. B) The fraction of single (non-overlapping) nanowires versus the number of nanowires in clumps is calculated for each Ni stripe length. Each data point represents cumulative data from 10 to 30 images, with approximately 50 nanowires per image.

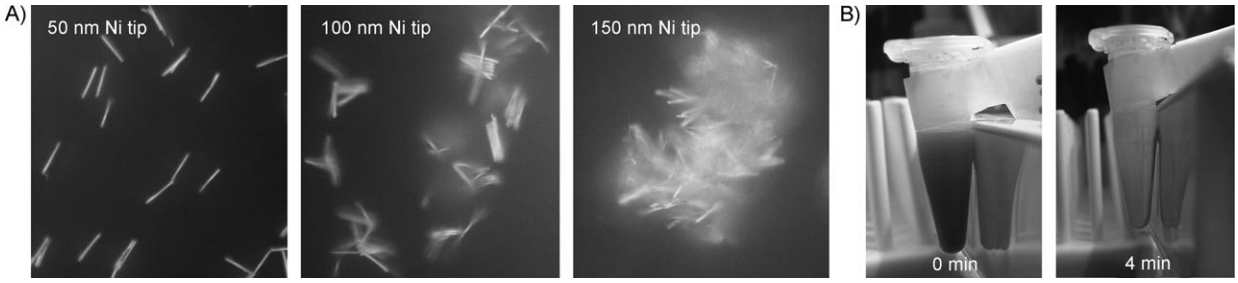

Figure 3. A) Images of the "residual magnetic clumping" effect on various Ni segments deposited at both ends of pure Au nanowires (stripe pattern 30000003; 0 = Au, 3 = Ni). The images were taken after the Ni nanowires were exposed to a Dynal Biotech magnetic strip for 30 min. Nanowires with Ni segments greater than 100 nm (total Ni amount is twice the stripe length) led to a marked increase in the residual clumping upon exposure to magnetic fields. B) Pictures of a suspended mixture of nanowires tipped with 50-nm Ni migrating towards a commercial Dynal magnetic strip after 4 min.

We also observed that electromagnets are equally efficient in the recovery process of the nanowires (data not shown), which is an important factor in our current efforts to fabricate a portable device to miniaturize the magnetic nanowire-based immunoassay on a fluidic card. While the present work focuses on demonstrating the nanowire-based immunoassay on a microfuge tube, our eventual goal is to use the magnetic properties of the nanowires to carry out an automated version of the assay within a fluidic card. Therefore, we performed tests to verify the ability to capture and isolate the nanowires by using reasonable magnetic fields. However, as a relatively high quantity of nanowires was utilized for the immunoassay in the present study (in a microfuge tube based assay rather than in a microscale system), they were recovered by the centrifugation process.

To ensure that the Ni segments at both ends of the nanowires do not affect the performance of Au- and Ag-striped nanowires in the immunoassay, a concentration-dependent titration experiment was repeated using the Ni-tipped nanowires against Bg spores and Ova proteins. The results obtained for the assays (data not shown) indicate that the LoD values observed for the two antigens studied are the same as those obtained when using the nonmagnetic nanowires. Hence, it was concluded that the presence of the flanking Ni tips does not affect the overall biosensing capabilities of the nanowires.

The development of biological nanosensors has been of interest lately as a result of their potential application in fundamental biology research and genetic screenings. In particular, both nanowires and nanorods have been recently reported to function as sensors, vehicles for gene delivery, and as nanotools for separating His-tagged proteins from underivatized proteins.[17–19] Here, we have demonstrated that metallic nanowires (both magnetic and nonmagnetic) can be employed as novel platforms for multiplex immunoassays. The described suspended array system takes advantage of the unique properties of these nanowires for efficient analysis (and potentially recovery) and holds much promise for novel diagnostic immunoassay platforms. The entire assay can be performed within 3–4 h, thus making it feasible to be employed on a rapid diagnostic platform. Ongoing work is focused on incorporating the assay onto a microfluidic device to allow for a portable biosensing system for biological warfare agents. The platform will ultimately enable an affordable and portable multiplex biodetection system for both first responders and clinicians such that the identity of the infectious agents can be accurately detected and confirmed, thus facilitating point-of-care applications.

Experimental Section

Surface Biofunctionalization: The nanowires were coated with a self-assembled monolayer of mercaptoundecanoic acid (MUA), which increased their dispersity and resulted in a functionalized surface of carboxylate groups that allowed the use of carbodiimide chemistry to attach primary amine groups of the capture antibody to the carboxylate groups on the nanowires. The nanowires were readily extracted from aqueous solution by quick centrifugation (5000 rpm × 1 min) and resuspended by sonicating and vortexing prior to use. The self-assembled MUA monolayers surrounding the nanowires were observed to be intact and functional for at least 1 year when the particles were stored in MUA-containing phosphate buffered saline (PBS; 10 mM, pH 7.4) at room temperature in a nitrogen storage box. Carboxylate-coated nanowires were conjugated to the capture antibody using 1-ethyl-3-(3-dimethylaminopropyl)carbodiimide (EDC; Pierce; Rockford, IL). Briefly, 100 μL of the stock suspension of the nanowires ($\approx 10^8$ particles) were washed twice with 100 μL of 2-morpholinoethanesulfonic acid (MES) buffer (50 mM, pH 4.5; Sigma, St. Louis, MO) and then resuspended in 145 μL of MES buffer (50 mM, pH 4.5) and 18 μL of the appropriate capture antibody (≈ 1 mg mL^{-1} stock concentration). The reaction vessel was placed on ice, and then 15 μL of EDC (20% w/v in 50 mM MES, pH 7.0) was added to the reaction mixture. The mixture was allowed to incubate at 4 °C with agitation for 1 h. Another 15 μL of EDC solution was subsequently added with an additional hour of incubation at room temperature. The antibody-derivatized nanowires were then washed once in 500 μL of PBS (10 mM, pH 7.4) containing 0.1% bovine serum albumin (BSA) and twice in 500 μL of PBS (10 mM, pH 7.4). The antibody-coated nanowires can be stored in 10 mM PBS (pH 7.4) at 4 °C for up to 2 months.

Multiplex Bioassay: 5 μL of each of the stock solutions of the selected Ab-conjugated nanowires ($\approx 10^5$ particles) was added to 100 μL of the antigen sample. The concentration ranges of the antigens tested are as follows: Bg spores at 1×10^8, 5×10^7, 1×10^7, 5×10^6, 1×10^6, 5×10^5, 1×10^5, 5×10^4, 1×10^4, 5×10^3, 1×10^3, and 0 cfu mL^{-1}; MS2 bacteriophage at 1×10^9, 5×10^8, 1×10^8, 5×10^7, 1×10^7, 5×10^6, 1×10^6, 5×10^5, 1×10^5, 5×10^4, 1×10^4, and 0 pfu mL^{-1}; and Ova protein at 10, 5, 1, 0.5, 0.1, 0.05, 0.01, and 0 mg mL^{-1}. The mixture was placed on a shaker and incubated for 30 min at room temperature. The particles were subsequently extracted by centrifugation (5000 rpm × 1 min), washed once in 100 μL of 10 mM PBS–0.1% BSA, and resuspended in 100 μL of a secondary reporter biotin-labeled antibody solution (5 μg mL^{-1} in 50 mM PBS) for 30 min. After two additional washes with 100 μL of PBS-BSA buffer, the nanowires were incubated with 15 μL of streptavidin–AlexaFluor647 fluorescent reporter conjugate solution (Molecular Probes, 5 mg mL^{-1} stock solutions) for 3 min. The particles were then extracted by centrifugation, washed twice with 10 mM PBS–0.1% BSA (pH 7.4), washed twice with 10 mM PBS containing Tween20 (0.05% v/v, pH 7.4), and resuspended in 100 μL of 5 mM PBS solution for imaging analysis.

Imaging and Data Analysis: Approximately 10^5 of the nanoparticles were placed in wells of a clear glass-bottomed 96-well microplate (MMI, Molecular Machines & Industries Gmbh; Eching, Germany) and imaged with a Zeiss Axiovert S100 inverted microscope equipped with a brightfield reflectance filter set (Chroma, 460/50X excitation, Q660LP dichroic, and 0.3ND) and AlexaFluor647 fluorescence filter set (HQ620/60X excitation, Q660LP dichroic, HQ700/75M emission) using a 63X oil immersion lens (NA = 1.4). The light source was a Lambda LS 300-W Xe arc lamp (LBLS/30 Sutter Instruments Inc., Novato, CA). Image acquisition consisted of collecting multiple image pairs (brightfield/fluorescence) over each well of the microplate. The reflectance image was used to delineate the stripe pattern (due to differential reflectivity) of the hexastriped Au/Ag nanoparticles, as each nanoparticle stripe pattern is matched with a particular ligand. The fluorescence images acquired over the same regions as the brightfield images were used to quantify the bound AlexaFluor647 fluorescent-labeled analyte of interest. Usually 25 reflectance and fluorescence image pairs (5 × 5) were acquired in a single well, taking less than 1 min to accomplish.

Received: March 21, 2006
Published online: August 4, 2006

Keywords: biological warfare · immunoassays · magnetic properties · nanotechnology · transition metals

[1] H. C. Lane, J. L. Montagne, A. S. Fauci, *Nat. Med.* **2001**, *7*, 1271.
[2] B. Durodie, *Curr. Opin. Biotechnol.* **2004**, *15*, 264.
[3] S. R. Nicewarner-Pena, R. G. Freeman, B. D. Reiss, L. He, D. J. Pena, I. D. Walton, R. Cromer, C. D. Keating, M. J. Natan, *Science* **2001**, *294*, 137.
[4] C. D. Keating, M. J. Natan, *Adv. Mater.* **2003**, *15*, 451.
[5] I. D. Walton, S. M. Norton, A. Balasingham, L. He, D. F. Oviso, Jr., D. Gupta, P. A. Raju, M. J. Natan, R. G. Freeman, *Anal. Chem.* **2002**, *74*, 2240.
[6] H. F. Finkel, X. Lou, C. Wang, L. He, *Anal. Chem.* **2004**, *76*, 353A.
[7] P. Gambardella, A. Dallmeyer, K. Maiti, M. C. Malagoli, W. Eberhardt, K. Kern, C. Carbone, *Nature* **2002**, *416*, 301.
[8] G. Iacob, O. Rotariu, N. J. C. Strachan, U. O. Hafeli, *Biorheology* **2004**, *41*, 599.
[9] A. Hultgren, M. Tanase, E. J. Felton, K. Bhadriraju, A. K. Salem, C. S. Chen, D. H. Reich, *Biotechnol. Prog.* **2005**, *21*, 509.
[10] M. Tanase, L. A. Bauer, A. Hultgren, D. M. Silevitch, L. Sun, D. H. Reich, P. C. Searson, G. J. Meyer, *Nano Lett.* **2001**, *1*, 155.
[11] M. T. McBride, D. Masquelier, B. J. Hindson, A. J. Makarewicz, S. Brown, K. Burris, T. Metz, R. G. Langlois, K. W. Tsang, R. Bryan, D. A. Anderson, K. S. Venkateswaran, F. P. Milanovich, B. W. Colston, Jr., *Anal. Chem.* **2003**, *75*, 5293.
[12] M. T. McBride, S. Gammon, M. Pitesky, T. W. O'Brien, T. Smith, J. Aldrich, R. G. Langlois, B. Colston, K. S. Venkateswaran, *Anal. Chem.* **2003**, *75*, 1924.
[13] R. S. Rao, M. T. McBride, J. S. Albala, D. L. Matthews, M. A. Coleman, *J. Proteome Res.* **2004**, *3*, 736.
[14] M. Chen, L. Siun, J. E. Bonevich, D. H. Reich, C. L. Chien, P. C. Searson, *Appl. Phys. Lett.* **2003**, *82*, 3310–3312.
[15] L. D. Garcia, L. C. Cheung, J. C. Mikkelsen Jr., J. G. Santiago, A. F. Bernhardt, V. Malba, *Proc. ASME Meeting* **2001**, 559.
[16] L. B. Bangs, *Pure Appl. Chem.* **1996**, *68*, 1973.
[17] S. G. Penn, L. He, M. J. Natan, *Curr. Opin. Chem. Biol.* **2003**, *7*, 609.
[18] A. K. Salem, P. C. Searson, K. W. Leong, *Nat. Mater.* **2003**, *2*, 668.
[19] K. B. Lee, S. Park, C. A. Mirkin, *Angew. Chem.* **2004**, *116*, 3110; *Angew. Chem. Int. Ed.* **2004**, *43*, 3048.

